

Lifetime study of sputtered PtAl coating on γ -TiAl with and without TBC topcoat at high temperatures

Authors: A. Ebach-Stahl¹, M. Fröhlich²

¹DLR – German Aerospace Center, Institute of Materials Research, 51170 Cologne, Germany

²University of Applied Sciences, 08056 Zwickau, Germany

Contact Information:

Corresponding author: Andrea Ebach-Stahl

DLR – German Aerospace Center

Institute of Materials Research

51170 Cologne, Germany

Email: andrea.ebach@dlr.de

Phone: +49 (0) 2203 601 2557

Maik Fröhlich:

University of Applied Sciences Zwickau

Faculty Physical Engineering / Informatics

Leupold Institute of Applied Sciences

Kornmarkt 1

08056 Zwickau, Germany

Email: maik.froehlich@fh-zwickau.de

Phone: +49 (0) 375 / 536 1508

Abstract

In this study, a PtAl based coating was tested under high temperature conditions at 900°C and 1000°C. The composition of Pt-53Al was chosen because of its excellent results in previous studies at another temperature. Due to the formation of a thin continuous alumina layer on top and the phase stability of the oxidation resistant coating, a lifetime of 1500 1h-cycles was achieved.

Depending on the testing temperature and time, the coating underwent an evolution of different Ti-Pt-Al phases due to the outward diffusion of Ti and Nb from the substrate and inward diffusion of Pt. The oxidation resistance decreases with a continued interdiffusion and a decreasing Pt content in the Ti-Pt-Al phases.

Additionally, the Pt-53Al coating was successfully deposited with a Thermal Barrier Coating top coat by EB-PVD. The oxidation test at 1000°C also revealed a lifetime up to 1500 cycles without failure, particularly based on the good adhesion between the TGO and TBC.

Mass gain measurements were done at each temperature and for all coating systems. Further microstructural examination methods to study the coating evolution, such as scanning electron microscopy (SEM), energy-dispersive X-ray spectroscopy (EDS) and X-ray diffractometry (XRD) for phase analysis, were used.

Keywords: PtAl; γ -TiAl; oxidation; coating; magnetron sputtering, 7YSZ

1. Introduction

Materials with a good oxidation and corrosion behavior are of high interest within the aerospace and automotive industry. State of the art Ni-based superalloys are used for components of aero and automotive engines as well as for gas turbines, which also provide attractive mechanical properties. Alumina former coating systems, such as MCrAlY (M=Ni and/or Co) [1-3] or Pt-modified aluminides [4-6], improve the oxidation resistance of the material.

However, mass reduction is one of the major goals for aeroengines. Light weight Titanium Aluminides, with their low density about 4g/cm^3 , are a material with attractive mechanical properties in a temperature range of $700\text{-}850^\circ\text{C}$ [7, 8]. A sufficient creep resistance can be provided up to 750°C [9], but above 750°C , a poor oxidation resistance characterizes this material due to the formation of fast growing and porous titania [10-12]. Therefore, an oxidation resistant coating is necessary to prevent material reduction by a fast oxidation process. Coatings based on the halogen effect [13-16] or sputtered coatings based on TiAl, TiAlCrZr/Y [16-21], as well as Si based coatings [22-24] show a positive effect on the oxidation behavior.

As shown in prior investigations, sputtered PtAl based coatings on γ -TiAl also provide an excellent oxidation resistance [25-28]. A thin and continuous Al_2O_3 layer was formed on top with a stable (Ti,Nb)PtAl₂ layer below. In this paper, further results of the oxidation resistance of sputtered PtAl-coatings on TiAl are presented. The lifetime and microstructure of the best coating composition of previous works, Pt-53Al [25], was tested at further temperatures, namely 900°C and 1000°C .

Additionally, the PtAl oxidation resistant coating was combined with a Thermal Barrier Coating (TBC) of yttria partially stabilized zirconia (7YSZ) on top within this study.

Currently 7 wt.% yttria partially stabilized zirconia is the industrial standard for TBCs on Ni-based superalloys. TBCs are widely used in aero-engines as well as land based gas turbines

due to their low thermal conductivity. A temperature reduction up to 150°C can be achieved for components with internal cooling [29-31]. Due to the application of ceramic top coats, the material beneath will be protected by operating at lower temperatures [32, 33]. Bondcoats with a good oxidation behavior, such as Al₂O₃ formation, provides good bonding between the TBC and substrate.

In this paper the coating system of a sputtered PtAl bondcoat with and without EB-PVD TBC consisted of 7YSZ was tested at testing temperatures of 900 and 1000°C.

2. Experimental

The γ -TiAl material (TNB V2) was provided by GfE (Germany) with the composition of Ti-45Al-8Nb-0,8C. Disc shaped specimens were machined with the dimensions of 15mm x 1mm. Before the coating procedure, the specimens were mechanical pretreated by the following steps: Grinding with SiC paper, polishing with a SiO₂ suspension and cleaning with ethanol.

The Pt-53Al coating was deposited by magnetron sputtering by using a two source equipment with the same process settings of previous experiments written in [25]. To get a homogeneous coating composition and thickness, the specimens were rotated in the coating chamber. The PtAl coating thicknesses were about 10 μ m. Afterwards, a cyclic test was performed at 900°C and 1000°C in air. One cycle consists of 60min heating time and 10min cooling down to 60°C. After 1500 cycles, the test was stopped. To study the microstructure evolution one sample was removed after 10, 100, 500, 1000 and 1500 cycles. The high test temperature of 1000°C was chosen to find the capability concerning the oxidation resistance.

Six Pt-53Al coated specimens were used to investigate the adhesion of a ceramic top coat. The thermal barrier coating (TBC) used within this study consisted of yttria partially stabilized zirconia (7YSZ). Before the TBC coating process via electron beam physical vapor deposition (EB-PVD), it is necessary to pre-oxidize the PtAl coatings to provide good adhesion. Therefore, the samples were oxidized at 950°C for 10h in air after magnetron sputtering. During the EB-PVD coating process, the samples were fixed on a planetary gear and the rotational speed was 4rpm. The sample temperature was approximately 950°C. The TBC-thickness was about 150 μ m. The samples with a TBC top coat were also tested cyclically at 1000°C up to 1500 cycles. Similar to the samples without a TBC top coat, one sample was removed after the aforementioned cycle states to investigate the microstructure. During the oxidation tests, the mass gain of each sample was recorded. The microstructure was examined for all samples by standard metallographic preparation of cross sections

followed by investigations at scanning electron microscopy (SEM; Zeiss Ultra 55) with energy-dispersive X-ray spectroscopy (EDS). Acceleration voltages of 3keV were used for image acquisitions and 20keV for EDS-analyses. For phase analysis, XRD measurements for selected samples were carried out using a Siemens D5000 powder diffractometer in Bragg-Brentano configuration with Cu K α radiation.

3. Results and discussion

3.1 Oxidation test at 900°C

The good oxidation behavior of the Pt-53Al coating at 950°C of previous investigations [25] was also verified at 900°C. The samples were tested up to 1500 cycles and the coating showed no signs of failure. In figure 1, the mass gain over exposure time is shown. The mass gain after 1500 cycles is very low (less than 0,5mg/cm²). Other comparable alumina forming coatings on TiAl, for example Ti-Al-Cr-Y, show a higher mass gain of about 1mg/cm² at 900°C after 1000 cycles [34].

During the thermal cyclic test, the PtAl coating underwent several phase transformations. All investigated TiPtAl-based phases (τ_2 , τ_3 and τ_4) are also described in [35, 36] and confirmed with XRD-measurements (figure 2). The chemical composition of the phases measured by EDS-analysis (seen in table 1) correlates to the data of the ternary Ti-Pt-Al phase diagram (figure 3, [35]).

Microstructure investigations show that within the first 10 cycles, a dense thin alumina layer with a thickness of about 300nm formed on top (figure 4a). Simultaneously the amorphous and homogeneous dense sputter coating crystallized. Beneath the thermally grown oxide (TGO) a huge area of PtAl and a two layer interface of one phase with the composition of TiPt₂Al and the τ_4 -TiPtAl phase were formed due to interdiffusion with the substrate. The mentioned TiPt₂Al-phase was only seen in the 10 cycle state. This phase could not be identified by XRD-measurements, however the peaks exist in the 10 cycles-diffractogram, which could not be collated to any other phases and disappeared after 100 cycles (figure 2). Maybe the peaks could have originated from this TiPt₂Al phase.

After 100 cycles the interdiffusion continued, so that the PtAl layer gets thinner underneath the TGO and a Pt₂Al₃ layer formed between the PtAl layer and the τ_4 -layer (figure 4b).

Although a relative high amount of Ti (11 at.%) and Nb (3 at.%) exists in this phase, the XRD-diffractogram clearly shows reflexes of Pt₂Al₃ (figure 2).

After 1500 cycles at 900°C, the TGO consisted of pure Al₂O₃ and only had a thickness of about 1-1.5µm. The PtAl-Bondcoat still existed with a thickness up to 20µm and consists of a layered structure of the τ₂, τ₃ and τ₄ phases. In figure 4c, the τ₂ phase is visible with the dark grey contrast and the τ₄ phase with the light grey contrast due to the higher amount of platinum. The τ₃ phase is not optical visible, but this phase has to exist in the τ₂-zones because EDS as well as XRD measurements show the existence of the τ₃ phase.

In the initial states of 900°C oxidation test the PtAl and Pt₂Al₃ phases and the later formed τ₂, τ₃ and τ₄ phases seem to be alumina formers. The solved Ti content in the PtAl and Pt₂Al₃ phases is relatively low in comparison to the other Pt-Al-based phases, so no oxidation of Ti took place. Presumably, the titanium in τ₂, τ₃ and τ₄ is bonded strongly enough, so no oxidation of titanium was seen until 1500 cycles. The exclusive alumina formation results in a very low oxidation rate.

Additionally the outward diffusion of Nb coming from the substrate was observed.

Apparently, the τ-phases have a relatively high stability against diffusion and does not solute a high amount of Nb, because the Nb-content did not exceed over 8 at.% after 1500 cycles at 900°C. TiAlNb-precipitates of a relative high Nb-content of about 20 at.% formed underneath the bondcoat, which confirm the conclusion of a relative low diffusion/solution of Nb in the PtAl-based phases.

3.2 Oxidation test at 1000°C

Even at high temperature of 1000°C the PtAl coating shows an excellent oxidation behavior. Unfortunately, it was not possible to record oxidation kinetics. Due to the given sample geometry (seen in figure 1), the mass gain curve of the PtAl coating system decreased after about 300 cycles. This mass loss is caused by a high oxidation rate and oxide spallation at the region where there is a hole in the samples that was not or insufficient coated for the massive oxidation attack at this high temperature of 1000°C. This hole, with a diameter of 1mm, is

necessary to fix the specimens during both coating processes and cyclic testing. Hence the substrate is locally not protected enough and oxidized rapidly at 1000°C. Although the oxidation kinetics of the 1000°C tests could not be continuously determined, it has been noted that the oxidation rate is very slow until spallation started after 300 cycles. In literature it is reported that mass gains for TiAlCrY based coatings on TiAl is about 1.2mg/cm² after 300 cycles without TBC at testing temperatures of 1000°C [34]. Thereby the mass gain of the PtAl coatings (about 0.6mg/cm²) is approximately half of the value of TiAlCrY coatings and also lower in comparison of halogen treated TiAl material (0.8 - 1.1 mg/cm²)[37].

At 1000°C the coating behavior is comparable to the 900 and 950°C test [25]. Due to the depletion of Pt by inward diffusion, a layer of PtAl precipitates was formed in a Pt₂Al₃ matrix in the upper part of the coating after 10 cycles (figure 5a). A double layer of τ_3 and τ_4 , developed by interdiffusion, was formed underneath Pt₂Al₃. After 100 cycles, due to further interdiffusion, the PtAl isles are solved and only the Pt₂Al₃, τ_2 and τ_3 were observed. Similar to the 900°C investigations, all mentioned phases were confirmed by XRD measurements as seen in figure 6 and the compositions are listed in table 2.

During the 1000°C-test, similar phase transformations occurred as in the 900°C test, so that after 1500 cycles, only the $\tau_2 + \tau_3$ phases exists underneath the TGO (figure 5b). In summary, within in the 1000°C test, the same phase transformations could be seen in comparison to lower testing temperatures with the difference being that the transformation rate was faster due to the higher temperature and therefore faster interdiffusion.

However, during the test TiO₂ also formed within the TGO at 1000°C. The formation of titania with the rutile modification started locally after 1000 cycles. With longer exposure time more interdiffusion took place. So that the TiPtAl-based phases destabilized and the oxidation of the fast growing titania was possible. Due to the fast oxidation of titanium and aluminum after phase destabilization, Pt precipitates stayed inside the thick oxide areas (figure 5b and XRD-diffractogram figure 6). Due to the small dimension of these precipitates,

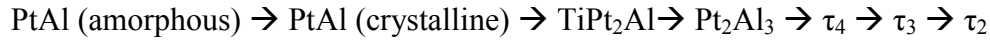
it could not be confidently determined if these precipitates were pure Pt or a kind of solid solution.

The effects of faster interdiffusion and phase transformation also can be seen in the XRD-diffractogram (figure 2+6). PtAl- and TiPt₂Al formed during the first cycles at 900°C were not seen in the 1000°C-diffractogram. Also the Pt₂Al₃, τ_3 and τ_4 phases, which were seen after 100 cycles at 900°C, already were measured after 10 cycles during the 1000°C test. Additionally the XRD-investigations showed TiO₂ + Pt peaks at samples tested at 1000°C after 1000 cycles.

The microstructural examinations revealed that the formation of local blistering already started occurring after 500cycles. In figure 5c, a micrograph of a blister is represented that formed after 1000 cycles. It seems that oxygen passed through various channels, for instance small cracks, and reacted with titanium of the previously mentioned destabilized TiPtAl-phases inside of the bondcoat. The fast growing titania needs more space and pushed the residual outer bondcoat outside and a blister was formed. Unfortunately parts of the formed titania broke out during cross section preparation, as seen in figure 5c.

Astonishingly, the blister formation did not have an essential negative effect on the lifetime. But although the Pt-53Al coating reached at least 1500 cycles of 1000°C without spallation of the coating or TGO, it can be seen that the closed protective alumina layer exists no longer. The oxidation resistance of the coating reached the technical limit concerning the oxidation resistance at this temperature due to the formation of fast growing titania. The most of the oxidation resistant Pt-53Al-coating was depleted due to diffusion and rapid oxidation.

By comparison of all investigation steps at every testing temperature in this study and the former investigations at 950°C [25], the following evolution of TiPtAl-phases can be conclude, starting from the amorphous PtAl coating after sputtering process. This evolution is verified by XRD-measurements (Figure 2 + 6):



First from the amorphous sputter coating, a crystalline PtAl bondcoat formed. In figure 4a + 5a, the PtAl and alumina phases can be seen after 10 cycles. Additionally, the Pt_2Al_3 phase formed at higher temperatures (950°C [25] and 1000°C) in the first cycles, presumably, due to the rapid Pt depletion of the faster Pt inward diffusion (figure 5a + 6).

Due to further interdiffusion (Pt inward diffusion and Ti/Nb outward diffusion), the next transformations steps are the formation of τ_4 , τ_3 and finally τ_2 before the fast oxidation of titanium started. In general the transformation rate depends on the temperature beside time and, therefore on the diffusion velocity.

3.3 Oxidation test at 1000°C with TBC

One major aim of this investigation was to elaborate whether a combination of a PtAl oxidation resistant coating with a thermal barrier top coat (TBC) of 7YSZ is feasible or not and if and how the TBC effects the oxidation behavior of the whole system.

Before applying the TBC by EB-PVD it was necessary to form a thin oxide scale to provide good adhesion of the ceramic top coat. Therefore, the samples were pre-oxidized for 10 hours at 950°C in air as noted in the “experimental” chapter.

Just as in the experiment without a TBC at 1000°C, the recording of oxidation kinetics was also difficult. Due to the weak point around the hole, fast oxidation took place with subsequent spallation of small TBC and oxide pieces after 250 cycles in this area. However, the general surface of the sample did not show any failure. The samples with TBC reached a lifetime of at least 1500 cycles which was the point where the test was stopped.

First microstructure investigations were performed directly after deposition of the TBC (figure 7a). Due to the pre-oxidation before top coat manufacturing, the samples phase

formation is similar to the 10 cycle state of the PtAl-coated samples without TBC. Beneath the TGO, Al₂O₃, a layered structure of PtAl, Pt₂Al₃ and τ_4 -TiPtAl formed. All element concentrations of the TiPtAl-based phases are listed in table 2.

The EB-PVD TBC was deposited with the typical columnar structure. Due to the smooth sample surface, the TBC grew up equally with a good adhesion to the pre-oxidized TGO (Al₂O₃).

After 1500 cycles at 1000°C, the PtAl coating was not completely oxidized, see figure 7b. Indeed a thick TGO of alumina and titania containing Pt-precipitates was formed, which remained after the oxidation of Al and Ti. Also the formation of pores was seen in the TGO. However, a thin dense alumina layer was seen beneath the TBC. This presence ensured a good adhesion of the TBC. Contrary to expectations no τ_2 -phase was seen, but a τ_4 -TiPtAl layer of about 5-10 μ m in thickness exists still after 1500 cycles between TGO and substrate. This behaviour has not yet been clarified.

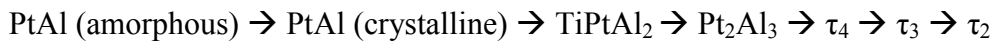
Due to the thickness of the TBC, no XRD measurements were done. All mentioned TiPtAl phases are based on the experience of the other XRD measurements without TBC and EDS investigations.

Additionally, it is to be seen that the TGO expands in the interspaces of the TBC due to the outward diffusion of titanium (figure 7b). This behavior of forming an inner and outer oxide scale is also reported in literature [38, 39], but the influence of this oxidation behavior is still not fully explained.

The blistering, which was seen after the 1000°C test at samples without TBC, could not be observed for samples with TBC topcoat. Areas of titania formation inside the intermetallic bondcoat were seen, but the TBC prevents the outward mechanical deformation of the coating. Feasible build internal stresses have no visible effect on the oxidation behavior and lifetime.

4. Summary

The oxidation resistance of a Pt-53Al-coating on γ -TiAl was investigated after cyclic testing at 900°C and 1000°C in air. Although the chosen testing temperatures were quite high for a γ -TiAl alloy, the present investigations prove the applicability of the coatings up to this technical limit. A lifetime of at least 1500 1h-cycles was observed. The formed alumina layer works as a barrier against the inward diffusion of oxygen and especially against the outward diffusion of titanium. This results in an excellent protection of the TiAl based material. During the thermal treatment, the amorphous Pt-53Al layer underwent several phase transformations according to the following scheme:



The transformations are depending on the exposure temperature and time and, therewith, on the diffusion rate of the elements involved.

The formation of titania with a rutile modification started locally after 1000 cycles at 1000°C. Presumably, the continuously decreasing Pt-content due to the Pt inward diffusion, leads to a destabilization of the TiPtAl based phases and are a reason for this unwanted oxidation behavior. In addition, blister formation was observed after 500 cycles caused by fast titanium oxidation inside the bondcoat.

Additionally, a Thermal Barrier Coating of 7YSZ was deposited on the PtAl bondcoat and tested at 1000°C successfully. The results, especially the phase formation and evolution during the test, are comparable to these without TBC at 1000°C. The TBC was still adhered after 1500 1h cycles without notable spallation, indicating an excellent adhesion and compatibility with this bond coat and the formed TGO.

Acknowledgment

We thank J. Brien, C. Kröder and D. Peters (German Aerospace Center, Institute of Materials Research) for the technical support and coating manufacturing. The authors acknowledge gratefully Prof. Dr. Uwe Schulz for the discussions and comments regarding this work.

References

1. Pint, B.A., et al., *Substrate and bond coat compositions: factors affecting alumina scale adhesion*. Materials Science and Engineering A, 1998. **245**: p. 201-211.
2. Schulz, U., et al., *Improvement of EB-PVD thermal barrier coatings by treatments of a vacuum plasma-sprayed bond coat*. Surface and Coatings Technology, 2008. **203**: p. 160-170.
3. Schulz, U., et al., *Influence of substrate material on oxidation behavior and cyclic lifetime of EB-PVD TBC systems*. Surface and Coatings Technology, 2001. **146-147**: p. 117-123.
4. Saint-Ramond, B., et al., *Low Mass Bondcoat for Robust Thermal Barrier Coatings*. Materials Science Forum, 2004. **461-464**: p. 265-272.
5. Brickey, M.R. and J.L. Lee, *Structural and Chemical Analyses of a Thermally Grown Oxide Scale in Thermal Barrier Coatings Containing a Platinum–Nickel–Aluminide Bondcoat*. Oxidation of Metals, 2000. **54**(3-4): p. 237-254.
6. Angenete, J. and K. Stiller, *Oxidation of Simple and Pt-Modified Aluminide Diffusion Coatings on Ni-Base Superalloys - II. Oxide Scale Failure*. Oxidation of Metals, 2003. **60**(1-2): p. 83-101.
7. Kestler, H. and H. Clemens, *Titanium and Titanium alloys* 2002: Wiley-VCH Verlag, Weinheim.
8. Clemens, H., et al. in *Ti 2003 Science and Technology*. 2003. Hamburg, Germany: Wiley-VCH Verlag, Weinheim.
9. Clemens, H. and S. Meyer, *Design, Processing, Microstructure, Properties, and Applications of Advanced Intermetallic TiAl Alloys*. Advanced Engineering Materials, 2013. **15**(4): p. 191-215.
10. Smarsly, W., et al. *Titanium Aluminides for Automotive and Gas Turbine Applications*. in *Structural Intermetallics*. 2001. Wyoming.
11. Brady, M.P., et al., *The Oxidation and Protection of Gamma Titanium Aluminides*. Journal of The Minerals, Metals & Materials Society 1996. **48**(11): p. 46-50.
12. Schmitz-Niederer, M. and M. Schütze, *The Oxidation Behavior of Several Ti-Al Alloys at 900°C in Air*. Oxidation of Metals, 1999. **48**(3-4): p. 225-240.

13. Donchev, A., R. Braun, and M. Schütze, *Optimizing Thermally Grown Oxide for Thermal Barrier Coatings on TiAl Components via Fluorine Treatment*. Journal of The Minerals, Metals & Materials Society, 2010. **62**(1): p. 70-74.
14. Donchev, A., B. Gleeson, and M. Schütze, *Thermodynamic considerations of the beneficial effect of halogens on the oxidation resistance of TiAl-based alloys*. Intermetallics, 2003. **11**: p. 387-398.
15. Friedle, S., et al., *Thermal barrier coatings on γ -TiAl protected by the halogen effect*. Surface and Coatings Technology, 2012. **212**: p. 72-78.
16. Pflumm, R., S. Friedle, and M. Schütze, *Oxidation protection of γ -TiAl-based alloys - A review*. Intermetallics, 2015. **56**: p. 1-14.
17. Zhou, C., et al., *Effect of Ti-Al-Cr coatings on the high temperature oxidation behavior of TiAl alloys*. Materials Science and Engineering A, 2001. **307**: p. 182-187.
18. Fröhlich, M., R. Braun, and C. Leyens, *Oxidation resistant coatings in combination with thermal barrier coatings on γ -TiAl alloys for high temperature applications*. Surface and Coatings Technology, 2006. **201**: p. 3911-3917.
19. Gauthier, V., et al., *Oxidation-Resistant Aluminide Coatings on γ -TiAl*. Oxidation of Metals, 2003. **59**(3-4): p. 233-255.
20. Liu, Z. and G. Wang, *Improvement of oxidation resistance of γ -TiAl At 800 and 900 C in air by TiAl₂ coatings*. Materials Science and Engineering A, 2005. **397**(1-2): p. 50-57.
21. Laska, N., R. Braun, and S. Knittel, *Oxidation behavior of protective Ti-Al-Cr based coatings applied on the γ -TiAl alloys Ti-48-2-2 and TNM-B1*. Surface and Coatings Technology, 2018. **349**: p. 347-356.
22. Ebach-Stahl, A., et al., *Improvement of the High-Temperature Oxidation Resistance of γ -TiAl by Selectively Pre-treated Si-based Coatings*. Advanced Engineering Materials, 2008. **10**(7): p. 675-677.
23. Xiong, H.-P., et al., *Formation of silicide coatings on the surface of a TiAl-based alloy and improvement in oxidation resistance*. Materials Science and Engineering A, 2005. **391**: p. 10-18.
24. Li, X.Y., et al., *Influence of siliconizing on the oxidation behavior of a γ -TiAl based alloy*. Intermetallics, 2003. **11**(2).

25. Ebach-Stahl, A. and M. Fröhlich, *Oxidation study of Pt–Al based coatings on γ -TiAl at 950 °C*. Surface and Coatings Technology, 2016. **287**: p. 20-24.
26. Das, D.K. and Z. Alam, *Cyclic oxidation behaviour of aluminide coatings on Ti-base alloy IMI-834 at 750 °C*. Surface and Coatings Technology, 2006. **201**: p. 3406-3414.
27. Das, D.K. and S.P. Trivedi, *Microstructure of diffusion aluminide coatings on Ti-base alloy IMI-834 and their cyclic oxidation behaviour at 650 °C*. Materials Science and Engineering A, 2004. **367**(1-2): p. 225-233.
28. Gurrappa, I. and A.K. Gogia, *High performance coatings for titanium alloys to protect against oxidation*. Surface and Coatings Technology, 2001. **139**: p. 216-221.
29. Gauthier, V., F. Dettenwanger, and M. Schütze, *Oxidation behavior of γ -TiAl coated with zirconia thermal barriers*. Intermetallics, 2002. **10**(7): p. 667-674.
30. Leyens, C., et al. *Environmental Protection of Gamma Titanium Aluminides*. in TMS. 2003. San Diego: The Minerals, Metals & Materials Society.
31. Leyens, C., et al., *Recent Progress in the coating Protection of Gamma Titanium-Aluminides*. Journal of Metals, 2006. **92**: p. 17-21.
32. Beele, W., G. Marijnissen, and A. van Lieshout, *The evolution of thermal barrier coatings — status and upcoming solutions for today's key issues*. Surface and Coatings Technology, 1999. **120-121**: p. 61-67.
33. Padture, N.P., M. Gell, and E.H. Jordan, *Thermal Barrier Coatings for Gas-Turbine Engine Applications*. Science, 2002. **296**: p. 280-284.
34. Laska, N. and R. Braun, *Lifetime of Thermal Barrier Coatings Deposited on γ -TiAl Based Alloys Using Intermetallic Ti–Al–Cr Bond Coats with Additions of Yttrium and Zirconium*. Oxidation of Metals, 2014. **81**(1-2): p. 83-93.
35. Raghavan, V., *Al-Pt-Ti (Aluminum-Platinum-Titanium)*. Journal of Phase Equilibria and Diffusion, 2010. **31**(1): p. 59.
36. Ding, J.J., et al., *Structural chemistry and phase relations in intermetallic systems Ti±{Pd,Pt}±Al*. Intermetallics, 2000. **8**(12): p. 1377-1384.
37. Laska, N., et al., *Lifetime of 7YSZ thermal barrier coatings deposited on fluorine-treated γ -TiAl-based TNM-B1 alloy*. Materials and Corrosion, 2016. **67**(11): p. 1185-1194.

38. Braun, R., et al., *Oxidation behaviour of gamma titanium aluminides with EB-PVD thermal barrier coatings exposed to air at 900 °C*. Surface and Coatings Technology, 2007. **202**: p. 676-680.
39. Braun, R., et al., *Thermally grown oxide scale on γ -TiAl coated with thermal protection systems*. Materials at High Temperatures, 2009. **26**(3): p. 305-316

Table I: Compositions of Ti-Pt-Al phases at 900°C; measured via EDS

| number of cycles | phase | concentration c [at.%] | | | |
|---------------------|------------------------------------|------------------------|-----|----|------|
| | | Al | Ti | Nb | Pt |
| 10 | PtAl | 44 | 4 | - | 52 |
| | TiPt ₂ Al | 25 | 26 | - | 49 |
| | τ_4 -(Ti,Nb)PtAl | 29 | 31 | 6 | 34 |
| 100 | PtAl | 54 | 0,5 | 5 | 40,5 |
| | Pt ₂ Al ₃ | 54 | 11 | 3 | 32 |
| | τ_4 -(Ti,Nb)PtAl | 31 | 29 | 7 | 33 |
| 1500 | τ_4 -(Ti,Nb)PtAl | 32 | 33 | 1 | 34 |
| | τ_2 -(Ti,Nb)PtAl ₂ | 45 | 29 | 2 | 24 |
| | τ_4 -(Ti,Nb)PtAl | 31 | 34 | 1 | 34 |
| | τ_2 / τ_3 | 39 | 28 | 8 | 25 |
| | τ_2 -(Ti,Nb)PtAl ₂ | 42 | 34 | 2 | 22 |

Table II: Compositions of Ti-Pt-Al phases at 1000°C; measured via EDS

| temperature 1000°C | number of cycles | phase | concentration c [at.%] | | | |
|---------------------------------|---------------------|--|--|-----|-----|------|
| | | | Al | Ti | Nb | Pt |
| without TBC | 10 | Pt ₂ Al ₃ | 55 | 11 | 3 | 31 |
| | | PtAl | 54,5 | 1,5 | 3 | 41 |
| | | τ ₃ | 36 | 29 | 10 | 25 |
| | | τ ₄ -(Ti,Nb)PtAl | 30 | 31 | 5 | 34 |
| | | Pt ₂ Al ₃ | 54,5 | 14 | 1,5 | 30 |
| | 100 | τ ₂ -(Ti,Nb)PtAl ₂ | 50 | 20 | 2,5 | 28,5 |
| | | τ ₃ | 38 | 32 | 8 | 22 |
| | | 1500 | τ ₂ -(Ti,Nb)PtAl ₂ | 46 | 16 | 9 |
| | τ ₃ | | 43 | 30 | 2 | 25 |
| | with TBC | as coated | PtAl | 54 | 2 | 2 |
| Pt ₂ Al ₃ | | | 52 | 13 | 2 | 33 |
| τ ₄ -(Ti,Nb)PtAl | | | 29 | 33 | 5 | 34 |
| 1500 | | τ ₄ -(Ti,Nb)PtAl | 31 | 31 | 3 | 35 |
| | | Nb-rich TiAl | 29 | 42 | 21 | 8 |

Figure captions

Figure 1: Mass changes of Pt-53Al coating on γ -TiAl at 900°C

Figure 2: XRD-diffractogram of PtAl coating after different cycles at 900°C

Figure 3: Ternary phase diagram Ti-Pt-Al leaned on [35] including measured EDS-data

Figure 4: SEM micrograph of Pt-53Al coating tested at 900°C

- a) 10 cycles
- b) 100 cycles
- c) 1500 cycles

Figure 5: SEM micrograph of Pt-53Al coating tested at 1000°C

- a) 10 cycles
- b) 1500 cycles
- c) Formation of blistering after 1000 cycles

Figure 6: XRD-diffractogram of PtAl coating after different cycles at 1000°C

Figure 7: SEM micrograph of Pt-53Al + TBC coating tested at 1000°C

- a) After TBC deposition
- b) 1500 cycles

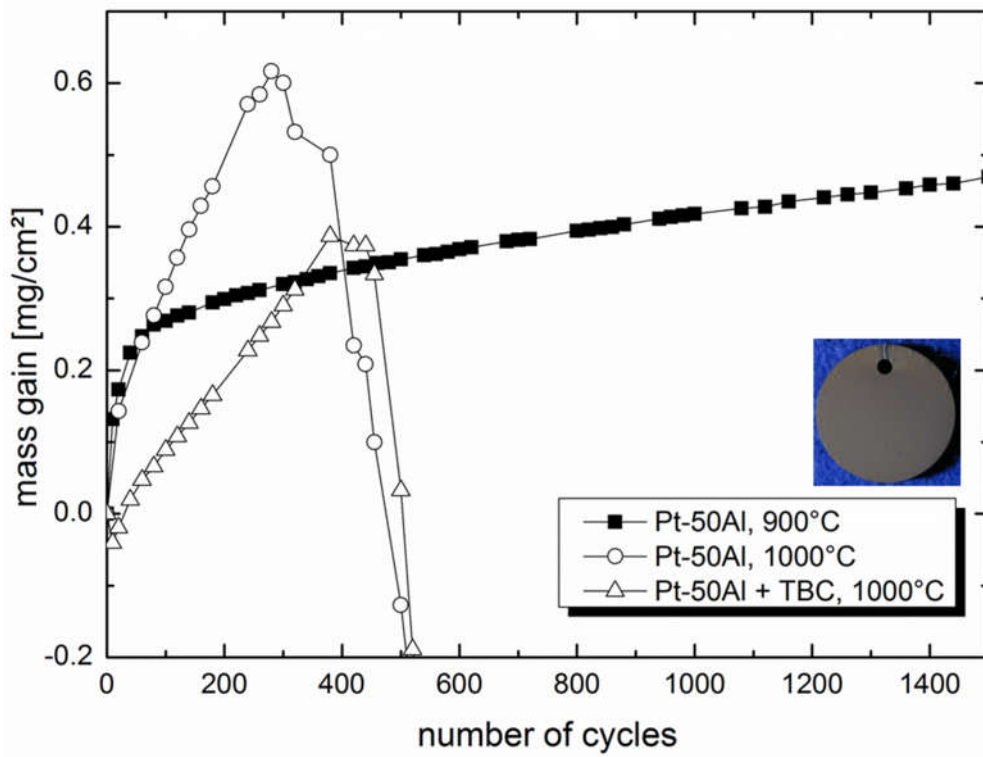


Figure 1

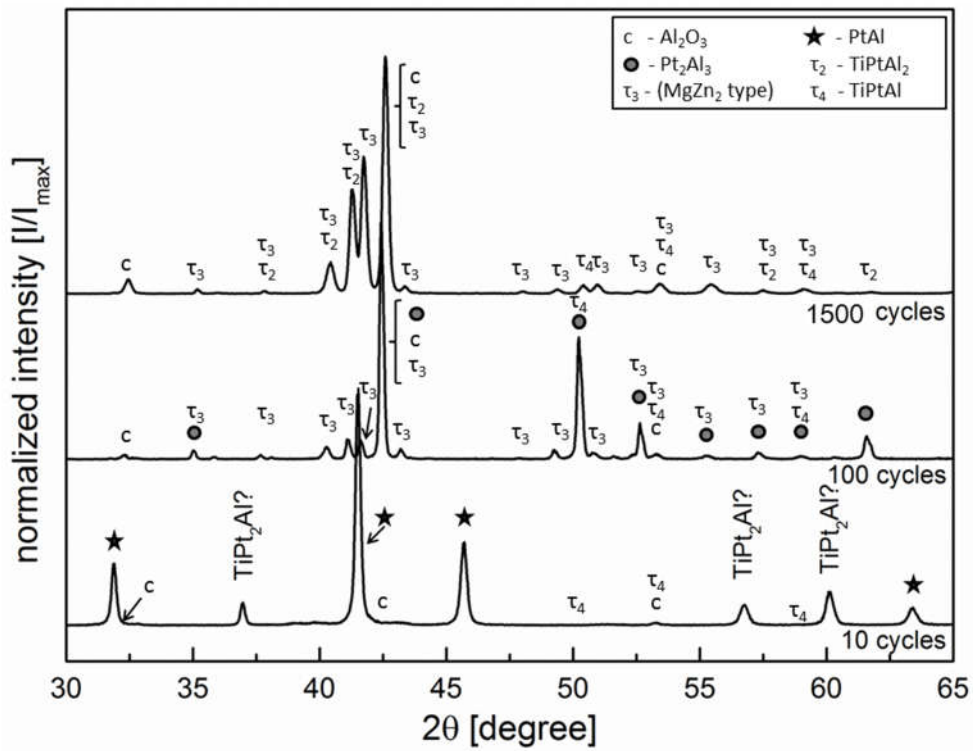


Figure 2

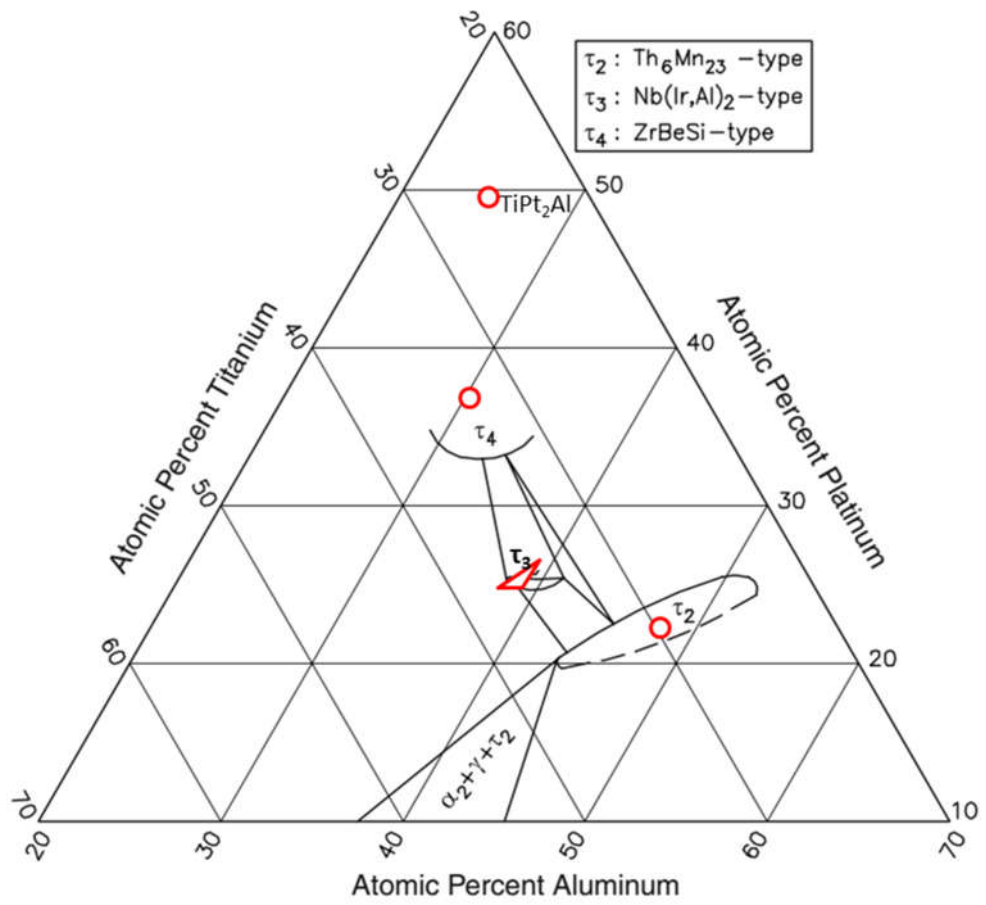


Figure 3

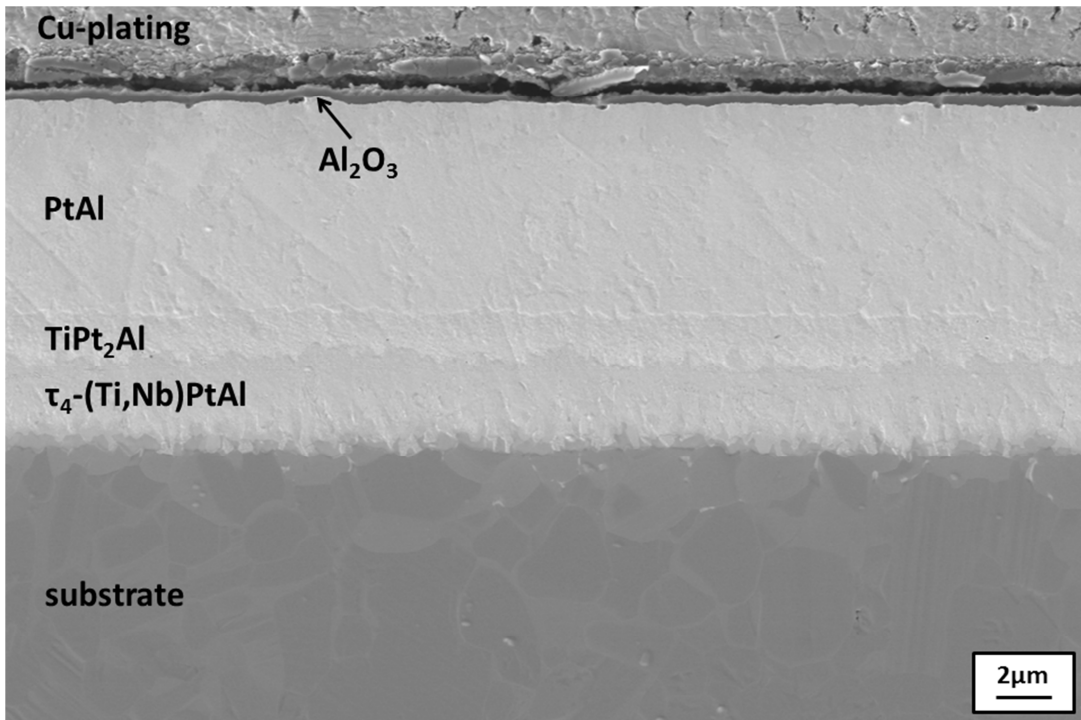


Figure 4a

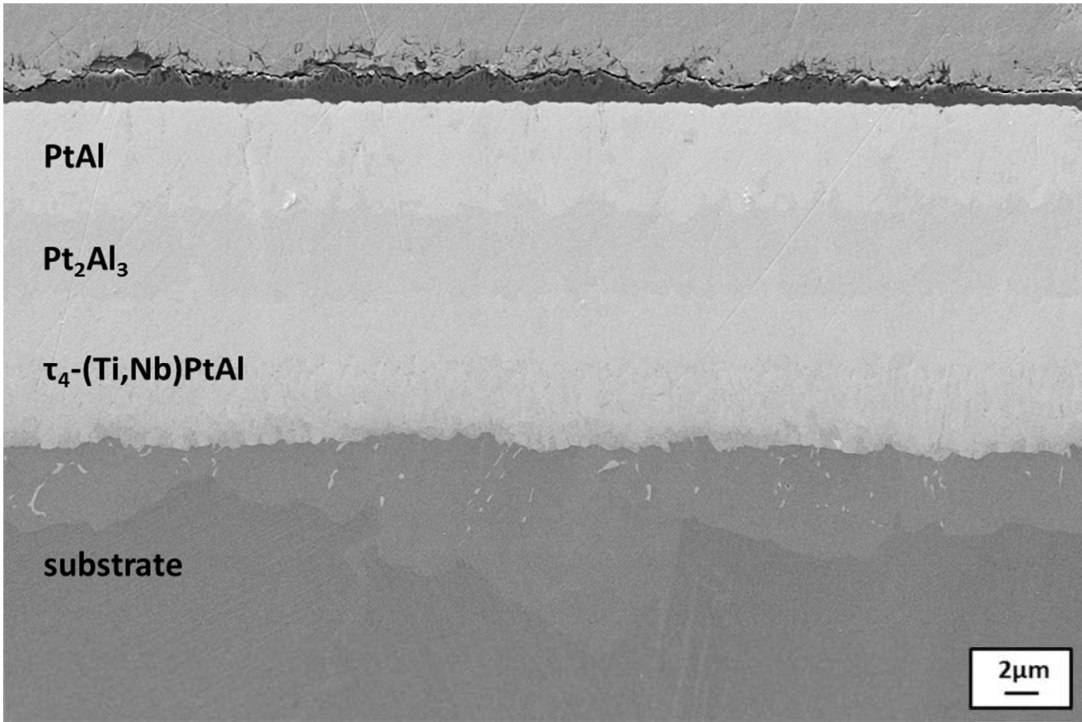


Figure 4b

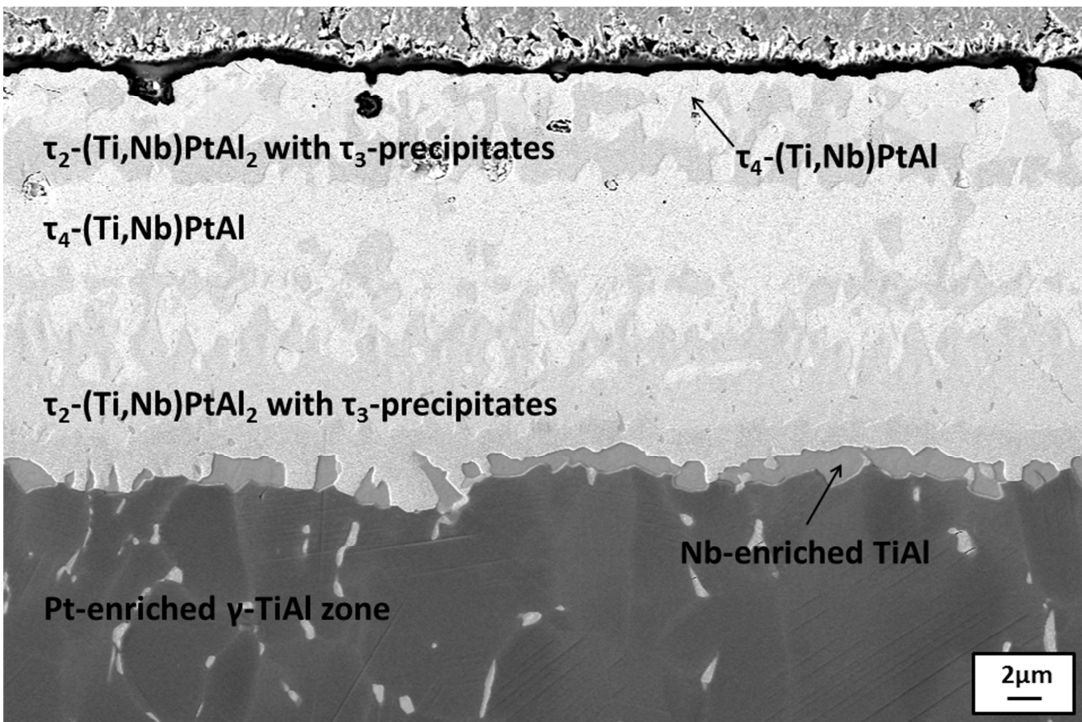


Figure 4c

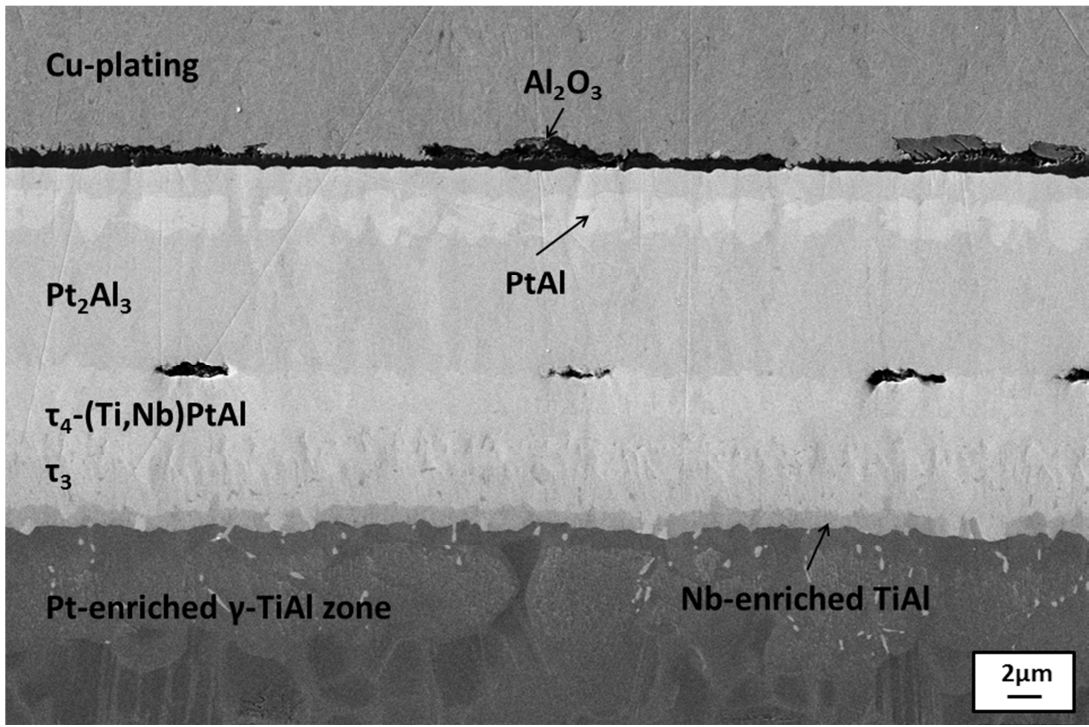


Figure 5a

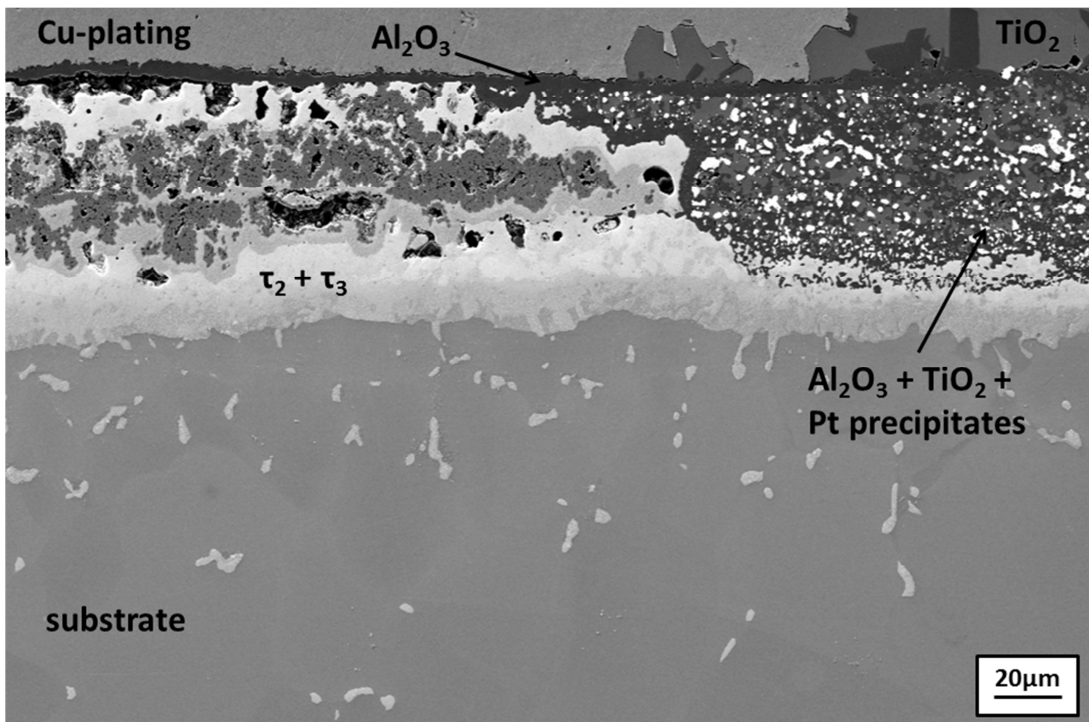


Figure 5b

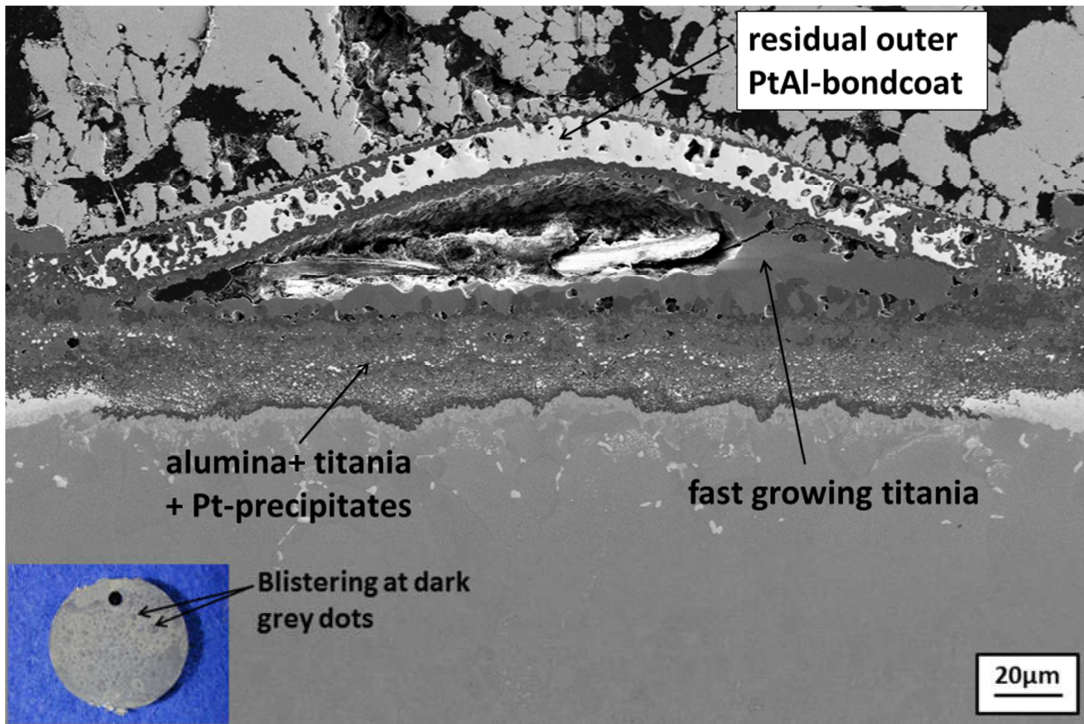


Figure 5c

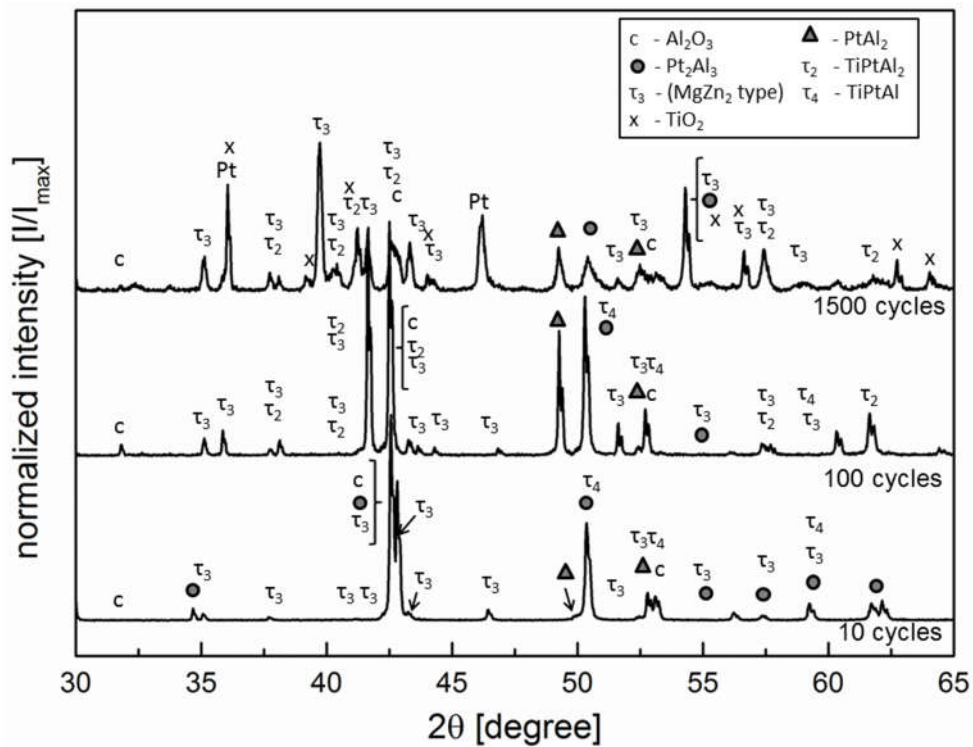


Figure 6

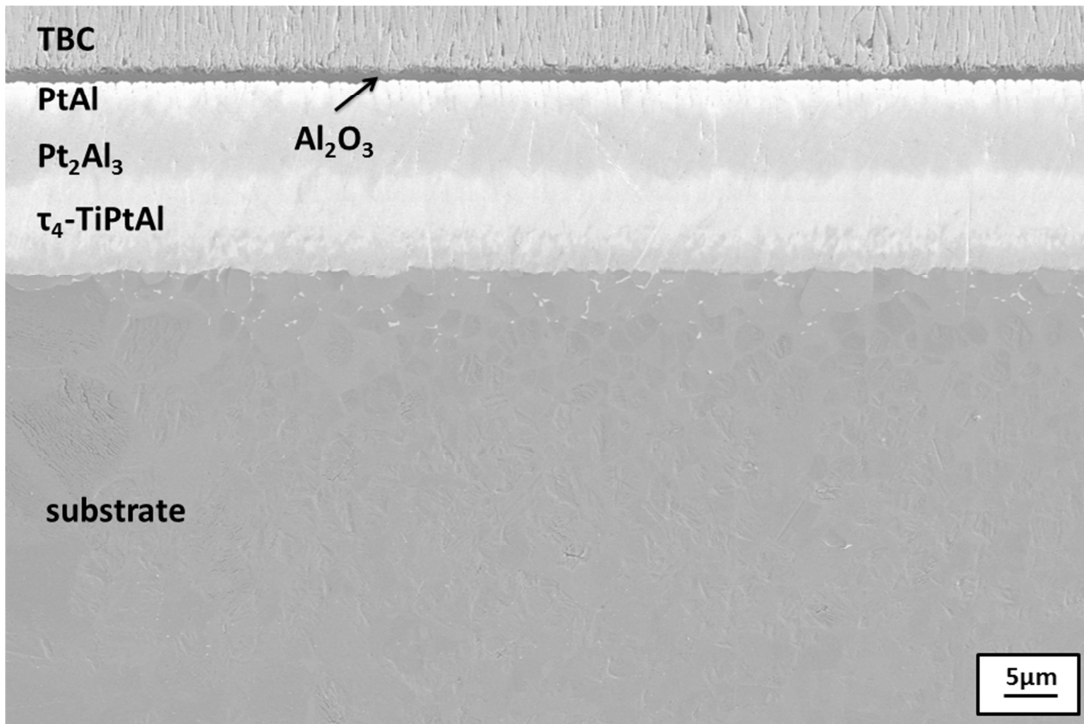


Figure 7a

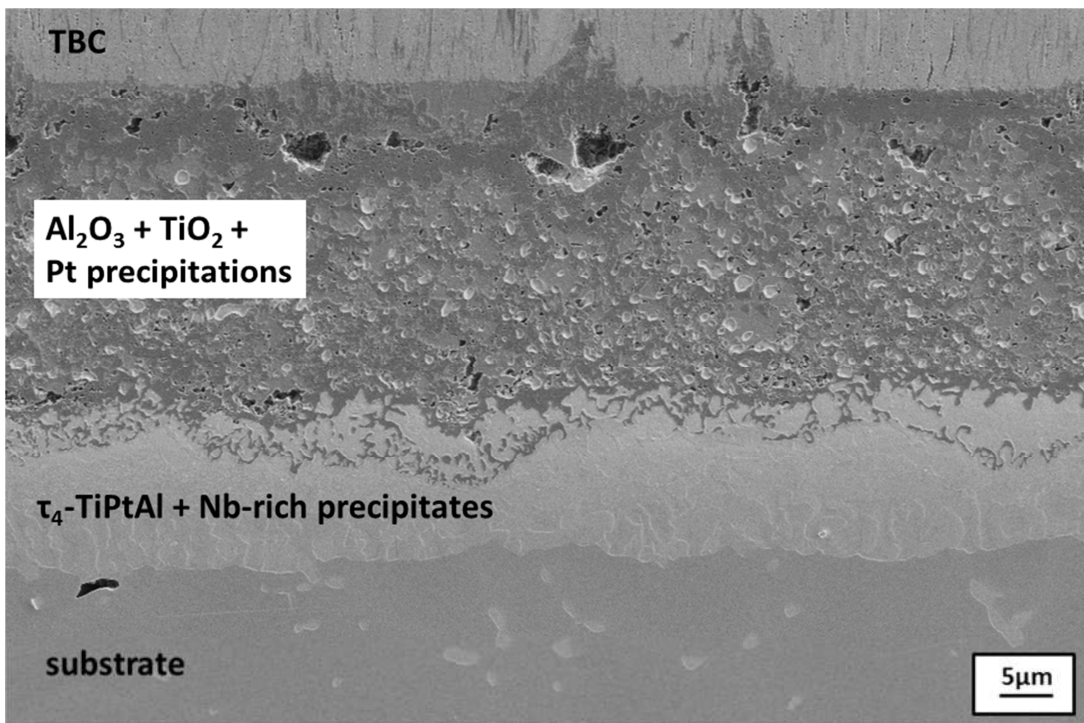


Figure 7b